AUTOMATIC SEGMENTATION OF THE DIAPHRAGM IN NON-CONTRAST CT IMAGES

Raja Yalamanchili[a], Deepak Chittajallu[a], Paul Balanca[a], Balaji Tamarappoo, MD[b], Daniel Berman, MD[b], Damini Dey, PhD[b], and Ioannis Kakadiaris, PhD[a]

[a]Computational Biomedicine Lab., Dept. of Computer Science, Univ. of Houston, Houston, TX
[b]Department of Imaging, Cedars-Sinai Medical Center, Los Angeles, CA

ABSTRACT

The diaphragm is a thin double-domed muscle that separates the thoracic and abdominal cavities. An accurate delineation of the diaphragm surface will be useful in providing a good region of interest for segmentation problems pertaining to the thoracic and abdominal cavities. In this paper, we present a fully automatic 3D graph-based method for the segmentation of the diaphragm in non-contrast CT data. In particular, we reformulate the diaphragm segmentation problem as an optimal surface segmentation problem in a volumetric graph. Comparison of the results obtained using our method with manual segmentations performed by an expert on non-contrast cardiac CT scans of 7 randomly selected patients indicated an overlap of $94.20 \pm 0.01\%$.

Index Terms— Diaphragm segmentation, non-contrast CT, max closure

1. INTRODUCTION

The diaphragm is a thin double-domed muscle that separates the thoracic and abdominal cavities. It is located below the lungs and forms the floor of the thoracic cavity on which the heart and lungs rest. An algorithm that is capable of accurately delineating the diaphragm surface can be used to obtain a good region of interest for the segmentation problems pertaining to the thoracic and abdominal cavities. However, automatic segmentation of the diaphragm in non-contrast CT data is challenging due to the similar appearance of organs surrounding the diaphragm and poor resolution of routinely acquired non-contrast CT scans.

Previous attempts to detect the diaphragm include semi-automatic [1] and automatic approaches [2] [3]. In the automated approach proposed by Zhou *et al.* [2], the diaphragm surface is estimated by deforming a thin-plane spline model to fit the bottom surfaces of the left and right lungs. One of the drawbacks of this approach is that it does not take advantage of any available edge information near the heart-diaphragm interface and the segmentation result obtained in these areas is purely driven by the smoothing constraints of the thin-plate spline. Rangayyan *et al.* [3] used a similar approach to obtain an initial estimation of the diaphragm surface and then followed it with a refinement step. Specifically, they used a quadratic surface to interpolate through the bottom surfaces of the left and right lungs and then used an active contour model to refine the diaphragm segmentation in each slice. The drawback of this approach is that the refinement step is purely done in 2D and does not use any inter-slice information.

In this paper, we present a fully automatic 3D graph-based method for the segmentation of the diaphragm in non-contrast CT data that utilizes both prior information about the anatomical location of the diaphragm and any available image information. In particular, we reformulate the problem as an optimal surface segmentation problem in a volumetric graph. Recently, Li *et al.* [4] proposed an efficient polynomial-time method for globally optimal surface segmentation in volumetric images. We adapt this method to solve our surface segmentation problem.

The rest of the paper is organized as follows: in Section 2, we present background material related to our work. In Section 3, we provide a detailed description of the proposed method for automatic segmentation of diaphragm. In Section 4, we present the results obtained using the proposed method and compare them with manual segmentations performed by an expert. Finally, in Section 5, we present our conclusions.

2. BACKGROUND

2.1. Minimum-cost closed set problem

Consider a directed graph $G = \langle V, E \rangle$, where E is the set of directed edges and $V = \{v_1, v_2, ..., v_n\}$ is the set of vertices or nodes. A closed set of the digraph G is defined as a set of n vertices $A \subset V$ such that if $v_i \in A$ and $(v_i, v_j) \in E$ then $v_j \in A$ (i.e., if a vertex v_i is in the closed set then all its successors are also in the closed set) which we refer to as the closure set constraint. Without loss of generality, let C be the cost function that associates each vertex $v_i \in V$ with a real numbered cost $C(v_i)$, which we abbreviate as C_i. Also, let $\mathbb{A}$ be the set of all possible non-empty closed sets of the digraph G. The cost of a closed set $A \in \mathbb{A}$ is defined as the sum of costs of all the nodes belonging to the closed set A. The minimum-cost closed set problem is then to search for a closed set $A^* \in \mathbb{A}$ with minimum cost. Formally, the *minimum-cost closed set problem* can be stated as:

$A^* = \arg\min_{A \in \mathbb{A}} \sum_{v_i \in A} C_i.$

The minimum-cost closed set problem can be re-formulated as an integer programming problem [5]. Let $x = \{x_1, ..., x_n\}$ be the set of membership variables where $x_i \in \{0, 1\}$ is the membership variable corresponding to the vertex v_i such that x_i is equal to 1 if $v_i \in A^*$ and 0 otherwise. Also, let e_{ij} be an indicator variable that is equal to 1 if $(v_i, v_j) \in E$ and 0 otherwise. According to the definition of a closed set, if $x_i = 1$ (i.e., $v_i \in A$) and $(v_i, v_j) \in E$ then $x_j = 1$ (i.e., $v_j \in A$), which is essentially the closure set constraint. It can be easily seen that this constraint is satisfied if $e_{ij} x_i (1 - x_j) = 0$. The minimum-cost closed problem is essentially equivalent to the following 0-1 integer programming problem:

$$\min_{x} \quad \left\{ \sum_{i=1}^{n} C_i x_i + \lambda \cdot \sum_{i=1}^{n} \sum_{j=1}^{n} e_{ij} x_i (1 - x_j) \right\} \qquad (1)$$

$$x_i \in \{0, 1\}, i = 1, 2, ..., n$$

where λ is set to a very high value (infinity) to ensure that the optimal solution satisfies the closure set constraint. The formulation expressed in equation 1 has the same form as the 0-1 programming formulation of a max-flow\min-cut problem [5]. The minimum-cost closed set problem can thus be solved in polynomial time by computing the $s - t$ mincut in a derived arc-weighted directed graph [5, 6].

2.2. Optimal surface segmentation as a minimum-cost closed problem

In this section, we briefly review the method proposed by Li *et al.* [4] for optimal single surface segmentation. The solution to the optimal surface segmentation problem is obtained by computing the minimum-cost closed set in a node-weighted directed graph. The key innovation of this method resides in the construction of the node-weighted directed graph that allows the transformation of the optimal surface segmentation problem into the problem of computing a minimum-cost closed set.

A volumetric image I can be viewed as a 3D matrix $I(x, y, z)$. The desired optimal surface in I is assumed to be terrain-like and oriented as shown in Fig. 1(a). Let N_x, N_y and N_z denote the size of the image I in x-, y- and z-dimensions, respectively. A feasible surface S in I is defined by a function $S : (x, y) \rightarrow S(x, y)$, where $x \in X = \{0, ..., N_x - 1\}$, $y \in Y = \{0, ..., N_y - 1\}$ and $S(x, y) \in Z = \{0, ..., N_z - 1\}$. Note that any feasible surface intersects with exactly one voxel of each column of voxels parallel to the z-axis, and the entire surface consists of exactly $N_x \times N_y$ voxels. The feasibility of a surface is further constrained by application-specific smoothing constraints enforced by two parameters, Δ_x and Δ_y, that are used to define the smoothness constraint along x- and y-directions, respectively. Specifically, if (x, y, z) and $(x+1, y, z')$ are two voxels on a feasible surface, then $|z - z'| \leq \Delta_x$. Similarly, if (x, y, z) and $(x, y + 1, z')$ are two voxels on a feasible surface, then $|z - z'| \leq \Delta_y$. Smaller values of Δ_x and Δ_y enforce stronger smoothing constraints on a feasible surface.

Let $c : (x, y, z) \rightarrow c(x, y, z)$ be a cost function that assigns a cost $c(x, y, z)$ to each voxel (x, y, z) in the image I. The cost $c(x, y, z)$ is an arbitrary real number that is inversely related to the likelihood that the desired surface contains the voxel (x, y, z). The cost of a feasible surface in I is then equal to the sum of the costs of all the voxels belonging to the surface. Thus, the optimal surface segmentation problem is to search for a feasible surface S^* with the minimum cost among the set of all feasible surfaces $\mathbb{S}$ definable in the image I. Specifically, the *optimal surface segmentation problem* can be stated as: $S^* = \arg\min_{S \in \mathbb{S}} \sum_x \sum_y c(x, y, S(x, y))$.

A node-weighted directed graph $G = \langle V, E \rangle$ is constructed to obtain a solution to the above-stated optimal surface segmentation problem as follows. Every voxel $(x, y, z) \in I$ is associated with a vertex $V(x, y, z)$ in the graph G. The cost or weight $w(x, y, z)$ assigned to the vertex $V(x, y, z)$ is defined as follows:

$$w(x, y, z) = \begin{cases} c(x, y, z) & \text{if } z = 0 \\ c(x, y, z) - c(x, y, z - 1) & otherwise. \end{cases} \qquad (2)$$

For each (x, y) pair in the image I such that $x \in X$ and $y \in Y$, we refer to the vertex-subset $\{V(x, y, z) | \forall z \in Z\}$ as the (x, y)-column of G and denote it by $Col(x, y)$. Two (x, y)-columns are considered to be adjacent if their corresponding (x, y) coordinates are neighbors under a given neighborhood system. For the purposes of this paper, we assume a 4-neighborhood setting. In this case, the column $Col(x, y)$ is adjacent to $Col(x + 1, y)$, $Col(x - 1, y)$, $Col(x, y + 1)$, and $Col(x, y - 1)$. The edge set E of the digraph G consists of two types of edges, *intra-column* edges and *inter-column* edges, which are defined as follows [4]:

- *intra-column edges:* Within each column $Col(x, y)$, every vertex $V(x, y, z)$, $z > 0$ has a directed edge to the vertex $V(x, y, z - 1)$.
- *inter-column edges:* Without loss of generality, consider two adjacent columns $Col(x, y)$, $x < N_x - 1$, and $Col(x + 1, y)$ along the x-direction. Each vertex $V(x, y, z) \in Col(x, y)$ is connected by a directed edge to the vertex $V(x + 1, y, max(0, z - \Delta_x)) \in Col(x + 1, y)$. Also, a directed edge is established from the vertex $V(x + 1, y, z) \in Col(x + 1, y)$ to the vertex $V(x, y, max(0, z - \Delta_x)) \in Col(x, y)$. Similar construction is performed for two adjacent columns along the y-direction. Figure 1(b) depicts the edges between the two adjacent columns along the x-direction. Note that these inter-column arcs are responsible for guaranteeing that if a voxel (x, y, z) is on a feasible

surface S, then its neighboring voxel $(x+1, y, z')$ on the surface S along the x-direction satisfies the required smoothness constraint, $|z - z'| \leq \Delta_x$. The same holds for two adjacent columns along the y-direction. Note that Δ_x and Δ_y must be greater than zero to allow the segmentation result to be a non-planar surface.

With the above-described graph-construction, it is easy to show that the minimum-cost closed set of the graph G solves the optimal surface segmentation problem.

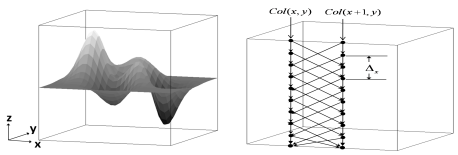

(a) (b)

Fig. 1. Optimal surface segmentation problem. (a) Depiction of orientation of the optimal surface, and (b) two adjacent columns along the x-direction of the constructed node-weighted digraph.

3. DIAPHRAGM SEGMENTATION

We reformulate the problem of diaphragm segmentation as an optimal surface segmentation problem to which the solution is obtained by computing the minimum-cost closed set in a node-weighted directed graph as described in Section 2.2. The key to achieving a good segmentation result to any given problem using the formulation detailed in Section 2.2 resides in the design of a good cost function $c(x, y, z)$ (Eq. 2) and in the incorporation of the appropriate smoothness constraints. We leverage prior information about the anatomical location of the diaphragm and any available image information in designing our cost function (Section 3.1). Additionally, we also modify the graph construction to introduce a soft planar smoothness constraint on the solution of the optimal surface segmentation problem (Section 3.2). Finally, as a post-processing step, we limit the scope of the segmentation result to the inner thoracic region which is obtained as described by Chittajallu *et al.* [7].

3.1. Cost Function

Based on prior knowledge about the anatomical location of the diaphragm, we require the optimal surface to pass through the set W_{LS} of voxels belonging to the bottom surface of the left and right lungs. In order to incorporate this prior knowledge, we first perform a rough segmentation of the lungs using simple thresholding and connected component analysis. Figure 2(b) depicts an overlay of the lung masks in a coronal slice of the non-contrast CT scan. We can then easily identify the set W_{LS} as the "bottom-most" voxels of the segmented lungs in each (x, y)-column. A very low cost must be assigned to these voxels in order to impose a hard constraint on the computed optimal surface to pass through these voxels. Additionally, a very high cost is assigned to set W_L composed of all the voxels inside the lung mask to stop the optimal surface from leaking into the lungs. In the case where none of the voxels in an (x, y)-column belong to the set W_{LS}, which occurs at the heart-diaphragm interface, we require the optimal surface to pass through the nearest fat-muscle transition. This can be captured by the presence of a strong z-gradient in that location. Additionally, our experiments with the response of various features at the heart-diaphragm interface indicate the local entropy to be most discriminative. However, entropy does not encode edge direction which is provided by the z-gradient. Figures 2(c,d) depict the z-gradient and the local Shannon entropy in a coronal slice. To take advantage of both, we impose hard constraints on the set W_E of all voxels with an entropy value greater than a certain threshold by assigning a very low cost. Based on the above considerations, we design the cost function as follows:

$$c(x,y,z) = \begin{cases} c_{min} & \text{if } (x,y,z) \in \{W_{LS} \bigcup W_E\}, \\ c_{max} & \text{if } (x,y,z) \in W_L, \\ -g_z(x,y,z) - c_{min} & otherwise. \end{cases} \tag{3}$$

where g_z denotes the absolute value of the z-gradient, with $c_{min} < min(-g_z)$ and $c_{max} > max(-g_z)$.

3.2. Modified Graph Construction

The smoothness of the solution obtained from the optimal surface segmentation problem can be controlled using the smoothness parameters Δ_x and Δ_y (see Section 2.2). The smaller the values of these parameters, the smoother will be the resulting surface. In general, smaller values are used for these parameters to stop the surface from jumping between any strong spurious edges in neighboring columns. However, if these spurious edges are located farther apart then there might be a scenario in which the optimal surface will pass through these edges in spite of setting smaller values for the smoothness parameters. This was precisely the problem that we experienced during our experiments. This demonstrated the need for a soft planar smoothness constraint to penalize the optimal surface whenever it deviates from being locally plane-like unless credible information is available about the presence of the diaphragm at that location. From the point of view of a minimum closed set problem, setting Δ_x and Δ_y equal to zero will force the optimal surface to be strictly a plane, which is not desired. Hence, in order to enforce a softer plane-like smoothness constraint, we migrate to the integer programming formulation of the minimum closed set problem (see Eq. 1). More clearly, we add planar inter-column edges between the voxel $V(x, y, z) \in Col(x, y)$ and its in-plane 4-neighbors $V(x+1, y, z) \in Col(x+1, y)$, $V(x-1, y, z) \in Col(x-1, y)$, $V(x, y+1, z) \in Col(x, y+1)$, and $V(x, y-1, z) \in Col(x, y-1)$. Let P be the set of these in-plane inter-column edges. We then use different values of

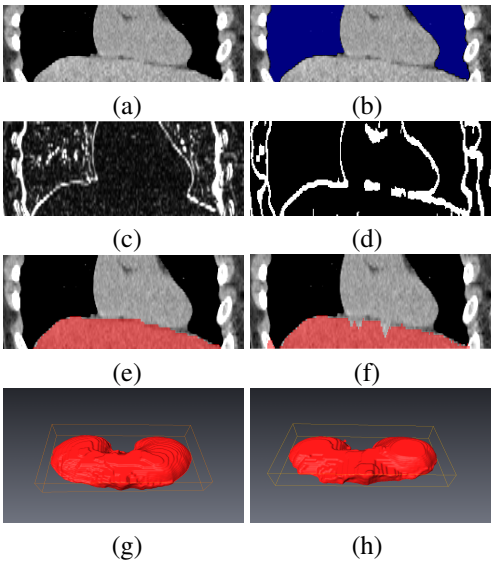

Fig. 2. Depiction of (a) raw Dicom Image, (b) Lung Mask (blue), (c) z-gradient, (d) entropy, and (e,f) segmentation results obtained with and without modified graph construction, respectively. (g,h) 3D Visualization of the diaphragm segmentation in two datasets.

λ in Eq. 1 for different edges in our graph. Specifically, we use a smaller value of λ (i.e., λ_p) for all the edges in the set P and we use a very high value (infinity) for all other edges of the graph. Doing so penalizes the optimal surface with a value $\lambda = \lambda_p$ at each location where it deviates from a plane locally.

4. RESULTS

We applied the proposed method on non-contrast cardiac EBCT scans of 7 randomly selected patients. Each CT scan has 50 to 60 axial slices with a pixel size of 0.68 *mm* $\times$ 0.68 *mm* and slice thickness of 3 *mm*. We evaluate the results of the proposed method by measuring their agreement/disagreement with manual segmentation performed by an expert. In Table 1, we depict the Dice similarity coefficient (DSC) and Hausdorff distance obtained using the proposed method. Figures 2(e,f) depict the segmentation result obtained in a coronal slice using our method with and without the modified graph construction described in Section 3.2. The "jumping" problem of the optimal surface discussed in Section 3.2 due to some spurious z-gradients can be observed in Fig. 2(f). Figures 2(g,h) depict 3D visualizations of the diaphragm segmentation in two datasets.

Table 1. Similarity and Dissimilarity measures

	DSC	Hausdorff Dist. *(mm)*
mean $\pm$ stddev	0.942 $\pm$ 0.010	18.339 $\pm$ 3.655
range	[0.922, 0.954]	[13.535, 23.542]

5. CONCLUSION

In this paper, we have presented a fully automatic graph-based method for the segmentation of the diaphragm in non-contrast cardiac CT data with very encouraging results. The proposed method can be easily adapted for the data from other imaging modalities (e.g., CTA and MRI).

6. ACKNOWLEDGEMENTS

This study was supported by NIH grant number R21EB006829-01A2 from the National Institute of Biomedical Imaging and Bioengineering (NIBIB) and the UH Eckhard Pfeiffer Endowment Fund. The content is solely the responsibility of the authors and does not necessarily represent the official views of the sponsors.

7. REFERENCES

[1] R. Beichel, G. Gotschuli, E. Sorantin, F.W. Leberl, and M. Sonka, "Diaphragm dome surface segmentation in CT data sets: A 3D active appearance model approach," in *Proc. SPIE International Symposium on Medical Imaging Image Processing*, San Diego, CA, Feb. 23-28 2002, vol. 4684, pp. 475–484.

[2] X. Zhou, H. Ninomiya, T. Hara, H. Fujita, R. Yokoyama, H. Chen, T. Kiryu, and H. Hoshi, "Automated estimation of the upper surface of the diaphragm in 3-D CT images," *IEEE Transactions on Biomedical Engineering*, vol. 55, no. 1, pp. 351–353, 2008.

[3] R.M. Rangayyan, R.H. Vu, and G.S. Boag, "Automatic delineation of the diaphragm in Computed Tomographic images," *Journal of Digital Imaging*, vol. 21, pp. 134–147, 2008.

[4] K. Li, X. Wu, D.Z. Chen, and M. Sonka, "Optimal surface segmentation in volumetric images: A graph-theoretic approach," *IEEE Transactions on Pattern Analysis and Machine Intelligence*, vol. 28, no. 1, pp. 119–134, 2006.

[5] J.-C. Picard, "Maximal closure of a graph and applications to combinatorial problems," *Management Science*, vol. 22, no. 11, pp. 1268–1272, 1976.

[6] Y. Boykov and V. Kolmogorov, "An experimental comparison of min-cut/max-flow algorithms for energy minimization in vision," *IEEE Transactions on Pattern Analysis and Machine Intelligence*, vol. 26, no. 9, pp. 1124–1137, 2004.

[7] D.R. Chittajallu, P. Balanca, and I.A. Kakadiaris, "Automatic delineation of the inner thoracic region in non-contrast CT data," in *Proc. 31st International Conference of the IEEE Engineering in Medicine and Biology Society*, Minneapolis, MN, Sep. 2-6 2009.